Adsorption 11: 147–157, 2005

A Theoretical and Experimental Study of Charge and Discharge Cycles in a Storage Vessel for Adsorbed Natural Gas

MOISÉS BASTOS-NETO, A. EURICO B. TORRES, DIANA C.S. AZEVEDO* AND CÉLIO L. CAVALCANTE JR.

Universidade Federal do Ceará, Departmento de Engenharia Química, Grupo de Pesquisas em Separações por Adsorção - GPSA, Campus do Pici, Bl. 709, Fortaleza, CE, Brazil, 60455-760

diana@gpsa.ufc.br

Received July 21, 2004; Revised June 2, 2005; Accepted August 2, 2005

Abstract. This study presents experimental data of storage and delivery tests of methane on activated carbon carried out in a prototype vessel at pressures up to 40 atm. Adsorption equilibrium data at high pressure were measured using a gravimetric apparatus. Experimental data obtained from the storage/delivery tests are compared to those obtained from process simulation using a dynamic model. The simulation model was run using the measured equilibrium data as input parameters. A good agreement was observed between experimental and simulated results. Histories of pressure and stored mass were satisfactorily well predicted. Despite heat effects, not precisely taken into account in the model, there was a reasonably good agreement between simulation and experiment for the average temperature inside the vessel.

Keywords: natural gas, activated carbon, storage and delivery, heat effects

1. Introduction

Natural gas (NG) is a non-renewable natural resource still available in great amounts and not totally used to its full energy potential. NG reserves are enough to supply the current demand for the next 60 years, twice as much as estimated for the oil reserves (Lozano-Castelló et al., 2002). Methane is the major constituent of natural gas, usually over 90% in volume. Among the paraffinic compounds, methane is the one with lowest normal boiling temperature (112 K). Moreover, its critical temperature is very low (192 K), so that it behaves approximately as an ideal gas at room temperature, even under high pressures. It has a spherical-symmetrical molecule without dipole or quadrupole moment, unlike other common adsorbates present in NG such as N_2 and CO_2, which have appreciable quadrupole moments. In view of this, methane can be adsorbed in adsorbents with apolar surfaces by means of van der Waals forces only.

Natural Gas is an attractive fuel for its cleaner combustion, which may potentially reduce CO, NO_x and SO_x emissions, especially in urban areas. However, natural gas use poses some disadvantages as compared to the liquid fossil fuels: it is relatively expensive to be transported to remote areas not served by gas pipelines and, under standard conditions of temperature and pressure, its energy density (defined as the combustion heat per volume unit) is only 0.038 MJ/l (0.11% of gasoline value), restricting its intensive use to areas served by gas pipelines. This has practically excluded natural gas from the transportation market, although the current concern with emissions from vehicles using liquid fuels has increased the interest for vehicles using natural gas as fuel. There is a considerable fleet of cars using compressed natural gas (CNG) with loading pressures around 20 MPa (Cook et al., 1999). Under these conditions, its density is about 230 times greater

*To whom all correspondence should be addressed.

than NG in normal conditions of temperature and pressure, usually referred to as 230 V/V. Thus, energy density of CNG at 20 MPa and 20°C is about 8.8 MJ/L, which accounts for 25% of the energy density of gasoline.

If natural gas is stored in the adsorbed form (ANG), the pressure reached in the reservoir may be considerably lower (about 3.5 to 4.0 MPa), which means lower costs with vessel construction and compression, besides greater safety. Another potential use of ANG is the transportation to remote areas with incipient demand not served by gas pipelines. Any material with pore diameter smaller than 2 nm (micropores, according to the definition of IUPAC—International Union of Pure and Applied Chemistry) is capable of adsorbing gases above their critical temperatures proportionally to the micropore volume. Activated carbons, because of the great micropore volume they may contain, have shown to be an appropriate material, which has been reported in most studies of ANG (Alcañiz-Monge et al., 1997; Cook et al., 1999; Cracknell et al., 1993; Menon and Komarneni, 1998; Parkyns and Quinn, 1995).

The storage of natural gas in adsorbed form inside vessels is subject to heat effects, which are much more pronounced than in the case of compressed gas. Since adsorption is an exothermic process, bed temperature rises during the charge, which results in a smaller storage capacity of gas in dynamic conditions. Likewise, temperature decreases in the discharge, which increases retention and hence lowers the amount of delivered gas. Under dynamic conditions, storage and delivery capacities are about 85 to 90% lower than those obtained on an ideally isothermal process. This capacity loss depends mainly in the shape of the adsorption isotherm curve. Besides, the thermal effects depend on the heat of adsorption, the heat transfer properties of the adsorbent bed and also on the heat exchanged through the walls of the vessel and with the atmosphere. Consequently, the performance and viability of an ANG system depends not only on the textural characteristics of the adsorbent, but also on the heat and mass transfer properties of the adsorbent bed and the storage vessel.

This study has the objective of showing experimental results for storage and delivery tests of methane carried out in a prototype vessel filled with activated carbon adsorbent. A dynamic model, which uses equilibrium data measured in our laboratory as input, is used to predict experimental data for vessel charge and discharge cycles with methane. A good agreement is observed between experimental and simulated results in terms of histories of pressure, temperature and stored mass.

2. Theory

The description of the charge and discharge cycle dynamics of an ANG reservoir has been the object of several studies in recent years (Biloé et al., 2002, 2001; Mota, 1999; Mota et al., 1997a, 1995; Pupier et al., 2005; Vasiliev et al., 2000). Modeling strategies are usually based on the formulation of mass and energy balances for the system, with a greater or lesser degree of sophistication in the description of hydrodynamics and mass/heat transfer involved.

The mathematical model used here to describe the process of natural gas charge and discharge in a bed of activated carbon considers the situation of local equilibrium of a single component. Thus, intra-particle and film resistances to mass and heat transfer are neglected. With this hypothesis, there is no need to apply distinct mass and energy balances for the non-adsorbed flowing phase and for the adsorbent.

On the other hand, a simple and efficient procedure to minimize the thermal effects is to allow that the gas flow in the bed be essentially radial (Chang and Talu, 1996). This can be achieved making the feeding or the discharge of the vessel through a small perforated cylinder installed in the center of the vessel.

The output variables of the storage vessel model are, therefore, $c(r, t)$, $T(r, t)$, $P(r, t)$ and $q(r, t)$, which are obtained from the simultaneous solution of the differential mass and energy balance equations, subject to the appropriate boundary and initial conditions imposed to the carbon bed.

Figure 1 shows a sketch of the system being modeled. It consists of a cylindrical tank packed with particles of a porous adsorbent. The gas enters and leaves the tank through a small perforated cylinder concentric to the larger cylinder, so that the flow of gas is essentially radial inside the cylinder.

We used a model based on that proposed by Mota et al. (1997b) with the following equations:

Continuity Equation:

$$\frac{\partial}{\partial t}(\varepsilon_c c + \rho_b q) + \nabla \cdot \vec{G} = 0 \qquad (1)$$

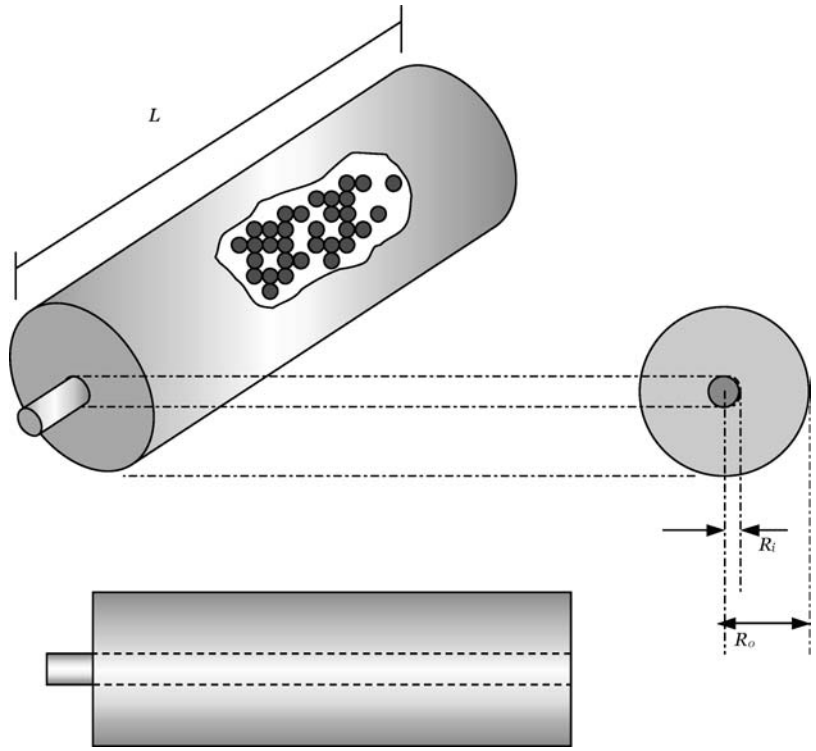

Figure 1. Model illustration.

Where $\vec{G}$ is the mass flux given by:

$$\vec{G} = \vec{v} \cdot c \tag{2}$$

Velocity is calculated by the Darcy's Law:

$$\vec{v} = -\frac{1}{\alpha}\nabla P \tag{3}$$

where α is the relationship between the gas viscosity and the bed permeability expressed by:

$$\alpha = \frac{150(1-\varepsilon_b)^2\mu}{4 \cdot \varepsilon_b^3 \cdot R_P^2} \tag{4}$$

Energy Equation:

$$\frac{\partial}{\partial t}((\varepsilon_c \cdot c + \rho_b \cdot q) \cdot C_{pg} \cdot T) + \rho_b \cdot \Delta H \frac{\partial q}{\partial t} - \frac{\partial P}{\partial t} + \rho_b \cdot C_{ps}\frac{\partial T}{\partial t} + \nabla \cdot (\vec{G} \cdot C_{pg} \cdot T - \lambda \cdot \nabla T) = 0 \tag{5}$$

The equilibrium relationship is given by a virial equation:

$$\frac{P}{q} = \exp\left(\left(k_1 + \frac{k_2}{T}\right) + \left(k_3 + \frac{k_4}{T}\right)q\right) \tag{6}$$

Initial conditions:

$$P = P_i, \quad T = T_i, \quad q = q(P_i, T_i) \quad \text{for} \quad R_i \le r \le R_0, \quad t = 0 \tag{7}$$

Boundary conditions:

$$\left.\frac{\partial P}{\partial r}\right|_r = 0 \quad \text{for} \quad r = R_0 \tag{8}$$

$$P = P_0, \quad \text{in } r = R_i \quad \text{for charge} \tag{9}$$

$$P = P_D, \quad \text{in } r = R_i \quad \text{for discharge} \tag{10}$$

$$\lambda_e \frac{\partial T}{\partial r} = c\frac{K}{\mu}\frac{\partial P}{\partial r}C_{pg}(T_w - T) \quad \text{for } r = R_i \tag{11}$$

$$\lambda_e \frac{\partial T}{\partial r} + e_w C_w \frac{\partial T}{\partial t} = h_w(T - T_{amb}) \quad \text{for} \quad r = R_0 \tag{12}$$

The algebraic-differential equations were solved by orthogonal collocation on finite elements using the solver gPROMS (Process System Enterprise Ltd., 1999).

The main characteristics of the carbon bed, such as the adsorption equilibrium isotherms, packing density, isosteric heat of adsorption, bed porosity and particle porosity were measured experimentally in our laboratory. The remaining parameters were either taken from the literature or estimated from correlations. They were the specific heat capacity of the solid (carbon), specific heat capacity of the gas, specific heat capacity of the vessel material, thermal conductivity of the bed and the heat transfer coefficient for convection in the external surface of the vessel.

3. Experimental

3.1. Materials

Granulated microporous activated carbon, WV1050, was kindly provided by Mead Westvaco (USA). Methane and helium purities were 99.5%vol.

3.2. Adsorption Isotherms

Methane equilibrium isotherms were measured gravimetrically with a magnetic suspension balance for high pressures (up to 15 MPa) by Rubotherm (Bochum, Germany). The experimental setup is depicted in Fig. 2. A sample of approximately 1.0 g was used, which was previously heated *in situ* at 150°C for about 12 hours. Specific volume of the sample was measured from helium measurements and the system characteristic volume was measured from a blank experiment (no sample) using methane. These volumes were used to account for buoyancy effects. Methane adsorption isotherms were measured in the pressure range of 0.1 to 7 MPa at 10, 20, 30, 40, 60 and 80°C. Details about the experimental procedure and buoyancy correction may be found elsewhere (Araújo, 2004).

3.3. Charge and Discharge Cycles

The experimental system for storage and delivery tests of methane was installed as shown in Fig. 3. The vessel

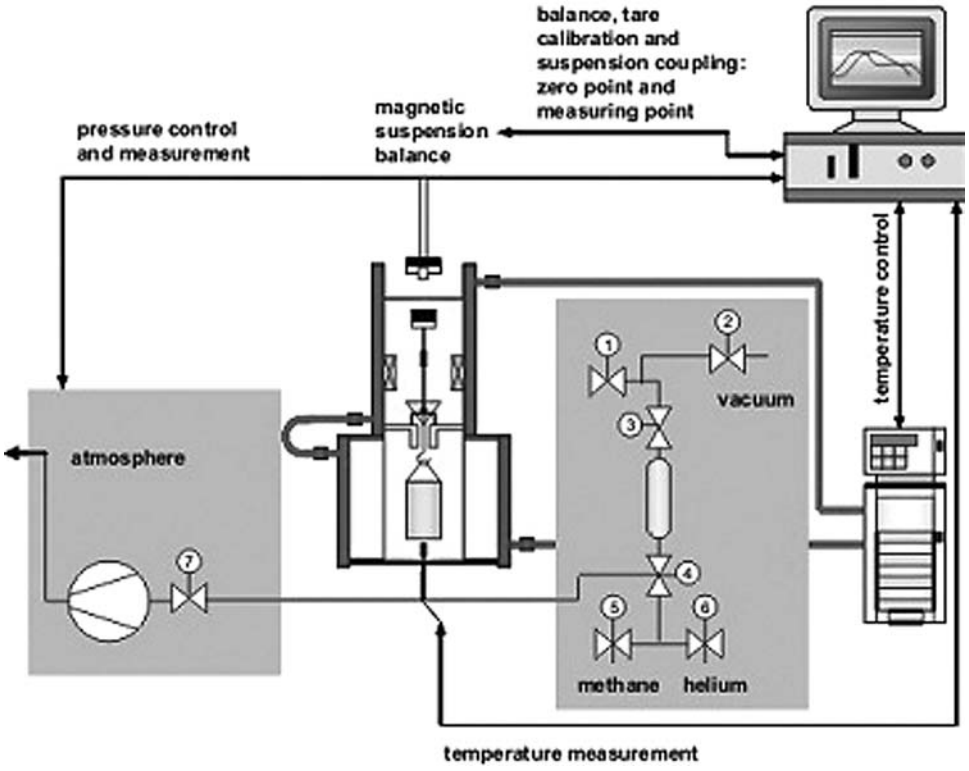

Figure 2. Experimental setup for equilibrium adsorption isotherms (Ustinov et al., 2002).

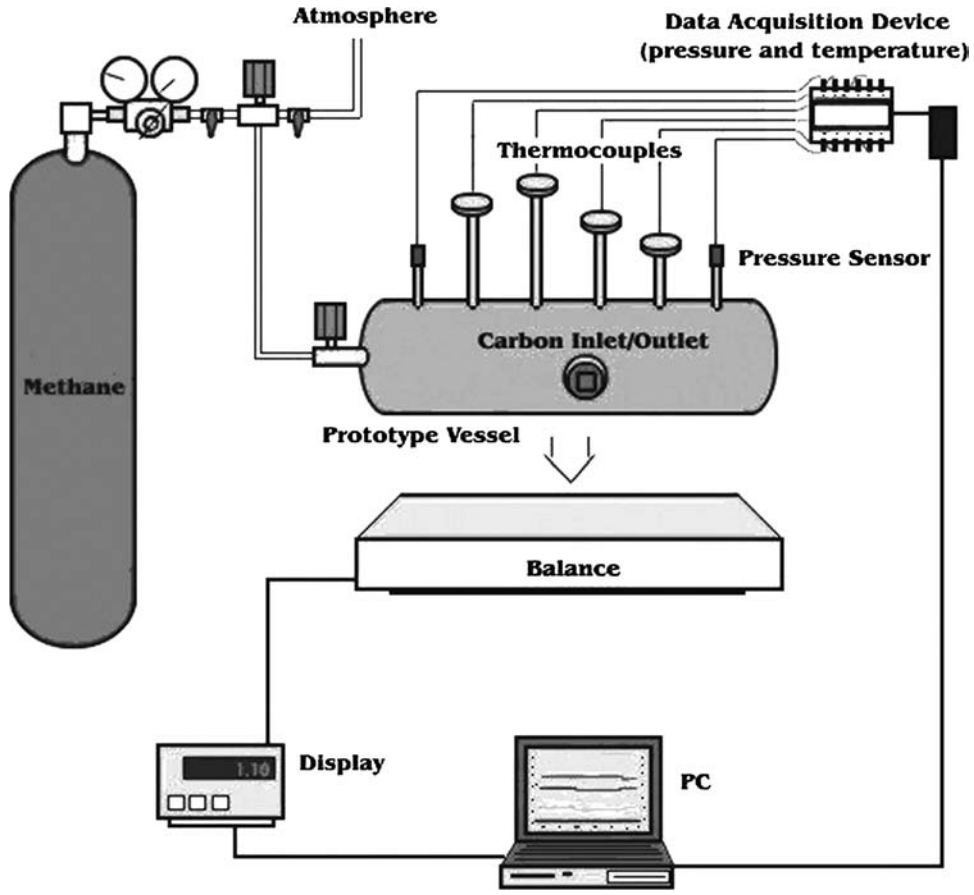

Figure 3. Experimental setup of prototype vessel.

was designed to withstand a pressure range of 0.1 to 4 MPa. It was made of carbon steel having the following dimensions: 0.003 m thickness, 1 m length and 0.20 m internal diameter. It was packed with approximately 10 kg of granulated activated carbon. Four thermocouples were placed along the vessel, about 12.7 cm far from one another and with radial coordinates of 14 mm, 39 mm, 64 mm and 89 mm in order to register the temperature distribution in the bed. Two pressure sensors were used to register the pressure inside the vessel in two different axial positions. The amount of stored gas was measured with a balance (Mettler) with 150 kg capacity and resolution of 50 g. An acquisition and registration system of the variables (temperature, pressure and stored mass) composed of a microprocessor unit and a data logger was used for real-time data acquisition.

The packing density of the carbon bed was calculated by measuring the necessary amount of carbon that would fill the prototype storage vessel and dividing it by its nominal volume (10 L).

The purpose of the experimental procedure used in the charge and discharge storage vessel was to register the behavior of the temperature, pressure and stored mass with time. The obtained data will be compared with the simulated results using the model presented previously.

The experimental procedure was established as follows:

(1) In the beginning of each run, the storage vessel was loaded with N_2 and then emptied with the aid of a vacuum pump. This procedure was performed at least three times in order to remove any gas previously adsorbed at the atmospheric pressure;
(2) After the temperature became stable inside the vessel, the valve of the methane bottle was adjusted for the pressure of 3.5 MPa;

(3) The vessel inlet valve was opened and the evolution of the monitored variables (pressure, temperature and stored mass) with time was registered;
(4) When the temperature became stable and homogeneous throughout the vessel, the valve of the gas bottle was closed and the flow of gas was diverted to the atmosphere, unloading the gas from the storage vessel. Again the evolution of the monitored variables was recorded;
(5) When the charge and discharge procedures were finished, reports with the recorded experimental data were obtained with purpose of comparing them to the simulated results.

4. Results and Discussion

4.1. Adsorption Isotherms

The equilibrium adsorption data measured for methane on Mead Westvaco activated carbon are shown in Fig. 4. They were plotted according to the linearized form of the virial equation. The data obtained at a given constant temperature fit into a straight line quite well. Isotherm parameters were calculated from the illustrated linear regression lines. Figure 5 shows the equilibrium isotherms obtained experimentally (points) as compared to each Virial equation with adjusted parameters. The adjusted parameters (k_1, k_2, k_3 and k_4) are shown in Table 1.

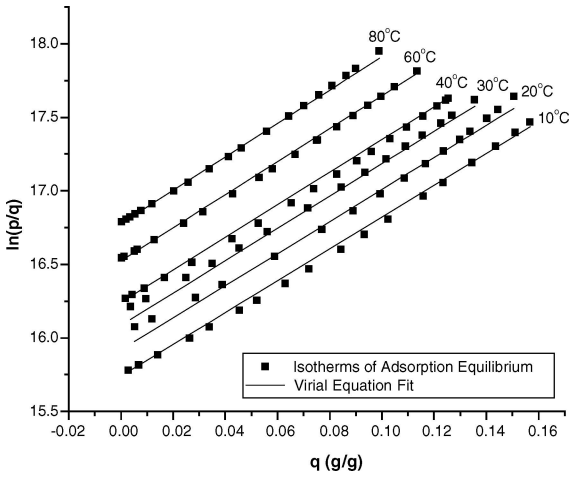

Figure 4. Virial equation fit for the adsorption isotherms of methane (10–80°C).

Table 1. Model input parameters.

C_{pg} (J/kg K)[d]	2450	R_0 (m)	0.103
C_{ps} (J/kg K)[b]	1375	R_i (m)	0.0127
C_w (J/m^3 K)	$3.92 \times 10^{+6}$	R_p (m)	0.5×10^{-3}
e_w (m)	0.003	T_{amb} (K)^{charge}	306
h_w (W/m^2 K)[b]	20	T_{amb} (K)^{discharge}	300
α (kg/m^3 s)	$150\mu\frac{(1-\varepsilon_b)^2}{\varepsilon_b^3 D_p^2}$	T_{eq} (K)	293 or 303
k_1[a]	20.9679	T_{ref} (K)	293
k_2[a]	−1480.27986	ΔH (J/kg)[a]	-975.31×10^3
k_3[a]	13.59576	ε_b[a]	0.592
k_4[a]	−788.31828	ε_c[a]	0.713
L (m)	0.90	λ (W/m K)[d]	0,212
M_g (kg/mol)	16.04×10^{-3}	μ (kg/m s)[c]	1.25×10^{-5}
P_0 (MPa) (typical value)	$3.66 \times 10^{+6}$	ρ_b (kg/m^3)[a]	280
P_{atm} (MPa)	$1.0131 \times 10^{+5}$	V_{pore} (cm^3/g)[a]	1.030
R (kJ/mol K)	8.3145	V_{mic} (cm^3/g)[a]	0.761

[a]Calculated in this study.
[b]Biloé et al. (2001).
[c]Mota et al. (1997b).
[d]Chang and Talu (1996).

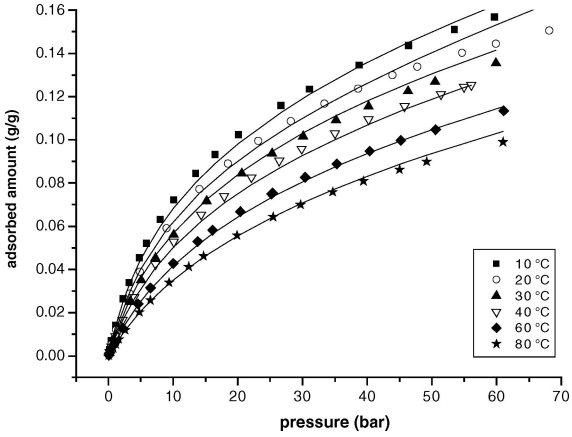

Figure 5. Adsorption isotherms of methane (10–80°C). Lines represent the virial fit of the experimental data.

4.2. Isosteric Heat of Adsorption

The equilibrium data was used to measure the isosteric heat of adsorption. Figure 6 shows the data obtained for constant values of adsorbed excess, m_{ex}, in terms of ln P versus 1/T. The adsorbed excess mass is defined as the weight change (measured by the balance) in equilibrium with a given pressure plus the corrections of buoyancy exerted on the specific volumes of the

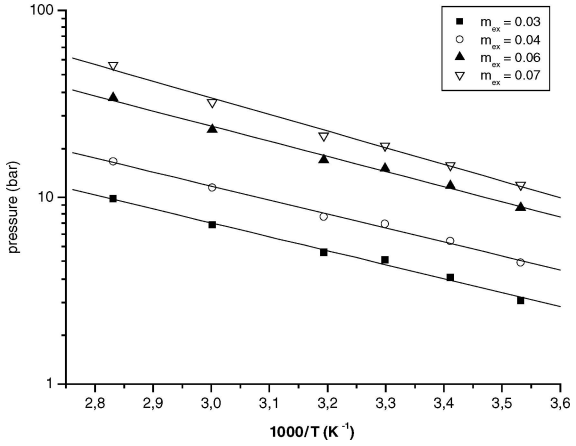

Figure 6. Adsorption isosteres of methane in activated carbon at 10, 20, 30, 40, 60 and 80°C. Lines represent the linear regression fit according to Eq. (13).

system and of the solid phase of the adsorbent sample (Dreisbach et al., 2002; Do and Do, 2003). The linear regression lines are included in Fig. 6 for each constant adsorbed excess mass. The isosteric heats of adsorption were calculated from the slope of these lines according to Eq. (13). Figure 7 shows the heats of adsorption obtained for four different adsorbed excess masses. The average heat of adsorption in the measured range is 15.61 kJ/mol. Note that the magnitude of the heat of adsorption increases significantly for an adsorbed excess mass above 0.04 g/g. However, for the sake of simplicity and conformity to the model equations, an average value was used.

$$\Delta H_{\text{ads}} = -R\left[\frac{\partial \ln p}{\partial(1/T)}\right]_{m_{\text{ex}}} \tag{13}$$

4.3. *Prototype Vessel Data*

Methane was charged into the prototype vessel, according to the experimental procedure previously described. During the loading cycle, the pressure measured in both sensors was approximately the same, indicating the high permeability of the porous media. The pressure increases quite fast, as may be seen in Fig. 8. The points are acquired experimental data whereas the curve was obtained from model simulation. The input parameter values used in the simulations are shown in Table 1. The model follows the experimental data quite closely, except for the very first initial points for which the model fails to reproduce the sharp spike in the pressure. This is due to the constant pressure boundary condition which does not reflect the fact that the system is in fact a constant pressure system if the flow is entering the tank, but when the solid + gas heat up backflow is not permitted and the pressure builds up.

Also, possible experimental errors in the calculation of the packing density may have been the cause of the initial mismatch. In other words, the real bed may be more loosely packed than the model assumes it to be. In fact, the packing procedure is performed by adding

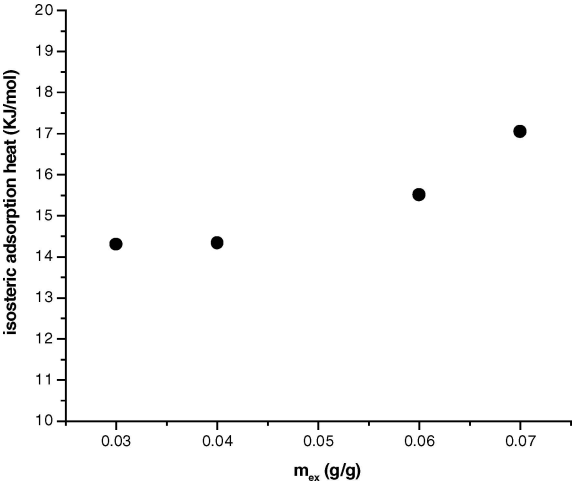

Figure 7. Isosteric heat of adsorption for methane in Westvaco activated carbon.

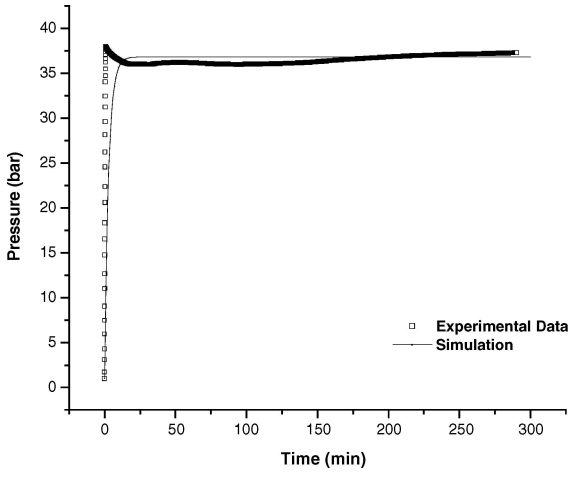

Figure 8. Experimental data and simulation for pressure inside the cylinder as function of time during the charge process.

the adsorbent into a central hole (see Fig. 3), followed by swinging and softly hammering the vessel. Unfortunately, there is no way of making sure that there are no undesired voids in the packing.

Figure 9(a) shows the average experimental temperature in the bed, which was calculated from the four temperature sensors located in different radial positions (see Fig. 9(b)). Simulated and experimental results match in the initial minutes and after 75 min. The simulated results, though, show a higher temperature increase than that obtained experimentally. This may be due to the variation of the heat of adsorption with the adsorbed mass, that was taken as an average value for simulation purposes. It is also an expected behavior if the model input parameter for packing density was actually larger than the real packing density of the prototype vessel. This last hypothesis is further confirmed in the plot of stored mass shown in Fig. 10. The measured stored amount in equilibrium was about 10% less than that predicted from the dynamic model, which may be due either to incomplete regeneration of the carbon bed or to a lower packing density.

When the temperature profiles inside the vessel leveled off, a discharge cycle was initiated by opening the inlet valve to the atmosphere (0.1 MPa). The two pressure sensors also measured approximately equal values throughout the run. Figure 11 shows the pressure

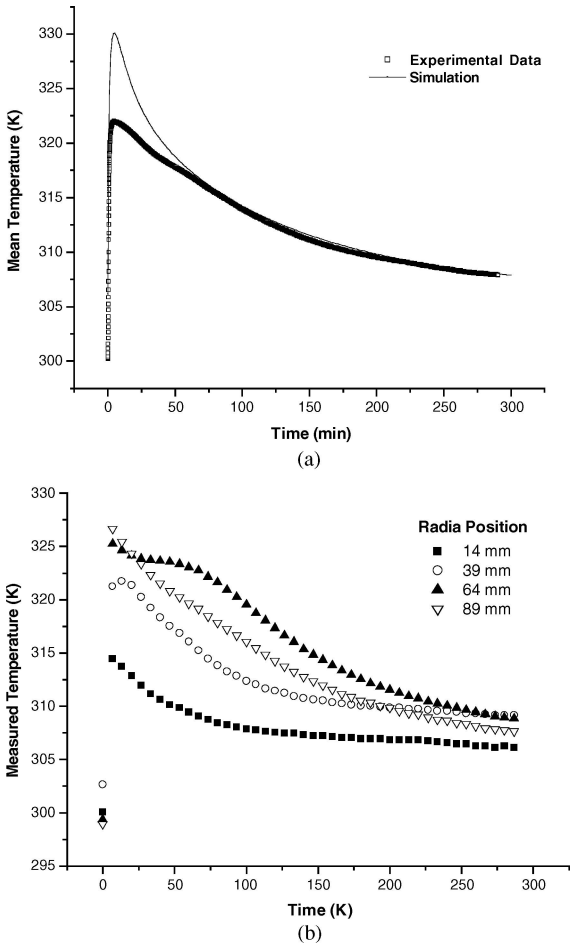

Figure 9. Temperature data for the charge process as function of time. (a) Experimental and simulation data for mean temperature inside the cylinder. (b) Experimental data for the temperature inside the cylinder measured with the four thermocouples.

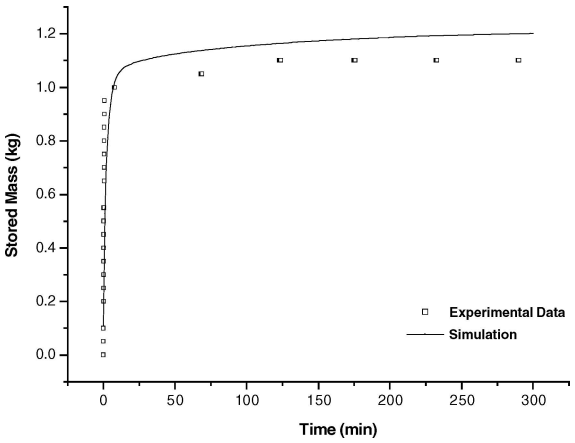

Figure 10. Experimental data and simulation for the amount of stored mass as function of time during the charge process.

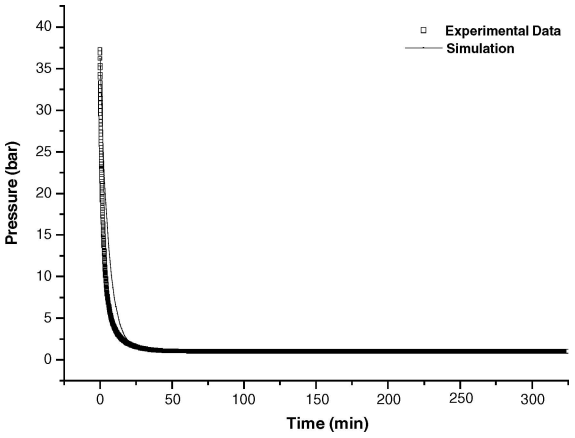

Figure 11. Experimental data and simulation for pressure inside the cylinder as function of time during the discharge process.

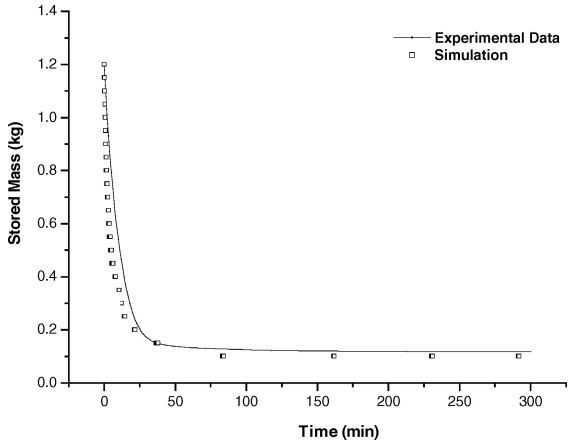

Figure 12. Experimental data and simulation for the amount of stored mass as function of time during the discharge process.

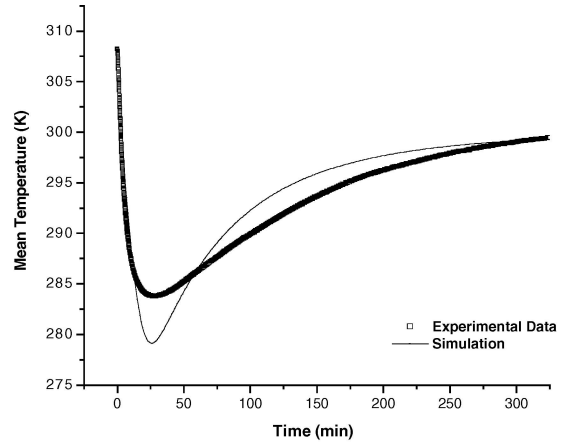

(a)

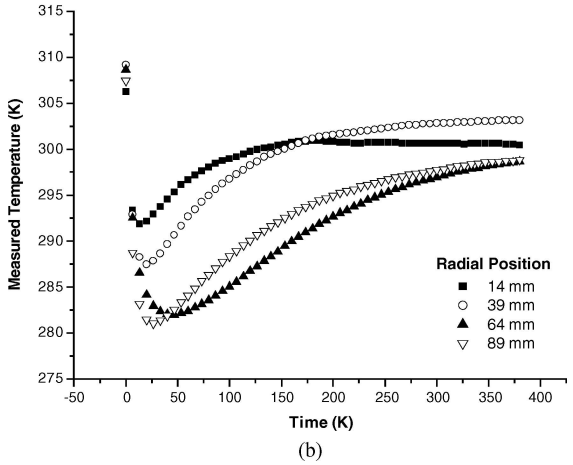

(b)

Figure 13. Temperature data for the discharge process as function of time. (a) Experimental and simulation data for mean temperature inside the cylinder. (b) Experimental data for the temperature inside the cylinder measured with the four thermocouples.

evolution measured by one of the sensors as compared to the simulated curve, which follows the experimental data very closely. Figure 12 shows the history of stored mass during discharge. A much nicer agreement between experimental and simulated data is observed. These evidences drawn from Figs. 11 and 12 suggest that the bed bulk density is actually correctly estimated, contrary to what was discussed for the charge results. The mismatch observed in the charging period is more likely to be due to heat effects. Figure 13(a) shows the average temperature inside the vessel during discharge, which was calculated as an average of the four temperature sensors (see Fig. 13(b). The experimental data qualitatively follow the simulated curve, but the maximum temperature difference is larger for simulated results similarly to the profiles measured for the vessel charge (see Fig. 9(a). This evidence highlights that heat effects not considered in the model may have an influence. These effects include (i) the variation of the adsorption heat with the adsorbed excess mass and (ii) the change in room temperature (which was not monitored in our experiment) during a cycle, which ordinarily lasts more than 5 hours. Future optimization of our model should involve these effects.

As a whole, however, it may be said that the model was able to qualitatively predict the measured experimental data of charge and discharge cycles. Note that the input parameters which were actually measured were essentially adsorption equilibrium parameters.

5. Conclusions

This study showed experimental loading and delivery tests of methane performed with a prototype storage vessel filled with microporous activated carbon. Equilibrium adsorption data were measured for the range of pressure and temperature of the system and used as the input information to a dynamic model for charge and discharge of the storage vessel. The experimental results were compared to simulated curves in terms of pressure, temperature and stored mass histories. There was a reasonably good agreement between simulation and experimental results despite possible heat effects not considered in the model: variation of heat of adsorption with loading and changes in room temperature throughout the experimental runs.

Nomenclature

c	fluid phase concentration, kg/m^3
C_{pg}	methane specific heat, J/kg K
C_{ps}	carbon specific heat, J/kg K
C_{w}	thermal capacity of the vessel wall, J/m^3 K
e_{w}	vessel wall thickness, m
$\vec{G}$	mass flux, kg/m^2 s
h_{w}	coefficient of heat transfer by convection, W/m^2 K
K	Darcy's equation parameter, kg/m^3 s
k_1, k_2, k_3 *e* k_4	parameters of virial isotherm of adsorption
L	vessel length, m
$\dot{m}$	gas mass flowrate, kg/s
m_{ex}	adsorbed excess mass per sample mass, g/g
M_{g}	methane molecular weight, kg/mol
P	pressure, Pa
P_0	final pressure on charge or initial pressure on discharge, Pa
P_{atm}	atmospheric pressure, Pa
P_{D}	final pressure on discharge or initial pressure on charge, Pa
P_{i}	initial pressure, Pa
q	adsorbed amount, kg/kg
R	universal constant of gases, kJ/mol K
R_0	outer radius of the vessel, m
R_{i}	inner radius of the vessel, m
R_{p}	adsorbent particle radius, m
T	temperature, K
t	time, s
T_{amb}	room temperature, K
T_{i}	initial temperature, K
t_{c}	cycle period, s
v	superficial velocity, m/s
ΔH	adsorption heat, kJ/kg

Greek Symbols

α	relationship between gas viscosity and bed permeability
ε_{b}	bed porosity
ε_{c}	porosity (void + macropores)
λ_{e}	thermal conductivity of the adsorbent, W/m K
μ	viscosity, kg/m s
ρ_{b}	packing density, kg/m^3

Acknowledgments

The authors acknowledge financial support from the sponsoring agencies FUNCAP, FINEP, CNPq, ANP and PETROBRAS.

References

Alcañiz-Monge, J., M.A. De la Casa-Lillo, D. Cazorla-Amorós, and A. Linares-Solano, "Methane Storage in Activated Carbon Fibres," *Carbon,* **35**(2), 291–297 (1997).

Araújo, J.C.S., *Estudo de Equilíbrio de Adsorção em Altas Pressões de Metano em Carvão Ativado,* M.Sc. Thesis, Fortaleza: Universidade Federal do Ceará, (2004).

Biloé, S., V. Goetz, and A. Guillot, "Optimal Design of an Activated Carbon for an Adsorbed Natural Gas Storage System," *Carbon,* **40**(8), 1295–1308 (2002).

Biloé, S., V. Goetz, and S. Mauran, "Dynamic Discharge and Performance of a New Adsorbent for Natural Gas Storage," *AIChE J.,* **47**(12), 2819–2830 (2001).

Cook, T.L., C. Komodromos, D.F. Quinn, and S. Ragan, In: T.D. Burchell, Editor, *Carbon Materials for Advanced Technologies*, Pergamon, New York, 269–302 (1999).

Cracknell, R.F., P. Gordon, and K.E. Gubbins, "Influence of Pore Geometry on the Design of Microporous Materials for Methane Storage," *J. Physical Chemistry,* **97**, 494–499 (1993).

Chang, K.J. and O. Talu, "Behavior and Performance of Adsorptive Natural Gas Storage Cylinders During Discharge," *Applied Thermal Engineering,* **16**(5), 359–374 (1996).

Do, D.D. and H.D. Do, "Adsorption of Supercritical Fluids in Non-Porous and Porous Carbons: Analysis of Adsorbed Phase Volume and Density," *Carbon,* **41**,(9), 1777–1791 (2003).

Dreisbach, F., H.W. Lösch, and P. Harting, "Highest Pressure Adsorption Equilibria Data: Measurement with Magnetic Suspension Balance and Analysis with a New Adsorbent/Adsorbate-Volume," *Adsorption,* **8**(2), 95–109 (2002).

Lozano-Castelló, D., J. Alcaniz-Monge, M.A. de la Casa-Lillo, D. Cazorla-Amorós, and A. Linares-Solano, "Advances in the Study of Methane Storage in Porous Carbonaceous Materials," *Fuel,* **81**(14), 1777–1803 (2002).

Menon, V.C. and S. Komarneni, "Porous Adsorbents for Vehicular Natural Gas Storage: A Review," *J. Porous Materials,* **5**, 43–58 (1998).

Mota, J.P.B., "Impact of Gas Composition on Natural Gas Storage by Adsorption," *AIChE J.,* **45**(5), 986–996 (1999).

Mota, J.P.B., A.E. Rodrigues, E. Saatdjian, and D. Tondeur, "Charge Dynamics of a Methane Adsorption Storage System: Intraparticle Diffusional Effects," *Adsorption,* **3**(2), 117–125 (1997a).

Mota, J.P.B., A.E. Rodrigues, E. Saatdjian, and D. Tondeur, "Dynamics of Natural Gas Adsorption Storage Systems Employing Activated Carbon," *Carbon,* **35**(9), 1259–1270 (1997b).

Mota, J.P.B., E. Saatdjian, D. Tondeur, and A.E. Rodrigues, "A Simulation Model of a High-Capacity Methane Adsorptive Storage System," *Adsorption,* **1**(1), 17–27 (1995).

Parkyns, N.D. and D.F. Quinn, in: J.W. Patrick, Editor, *Porosity in Carbons*, Edward Arnold, London, 293–325 (1995).

Process System Enterprise Ltd. gPROMS v1.7 User Guide., London, 1999.

Pupier, O., V. Goetz, and R. Fiscal, "Effect of Cycling Operations on an Adsorbed Natural Gas Storage," *Chemical Engineering and Processing,* **44**(1), 71–79 (2005).

Vasiliev, L.L., L.E. Kanonchik, D.A. Mishkinis, and M.I. Rabetsky, "Adsorbed Natural Gas Storage and Transportation Vessels," *Int. J. Thermal Sciences,* **39**(9–11), 1047–1055 (2000).

Ustinov, E.A., D.D. Do, A. Herbst, R. Staudt, and P. Harting, "Modeling of Gas Adsorption Equilibrium over a Wide Range of Pressure: A Thermodynamic Approach Based on Equation of State," *J. Colloid and Interface Science,* **250**, 49–62 (2002).